

Supplementary Material

The synergism between self-activated and impurity-related emissions of $\text{LiCa}_3\text{ZnV}_3\text{O}_{12}$: lattice distortion, energy transfer and temperature sensing effect

Jie Li ^a, Qian Ma, Ruixia Shi, Yongqiang Cao, Ling Chen, Aiyu Zhang^{a*}, and Ping Yang^{a*}

School of Material Science and Engineering, University of Jinan, 250022, Jinan, China.

Corresponding author. E-mail address: mse_zhangay@ujn.edu.cn (A.Y. Zhang),

mse_yangp@ujn.edu.cn (P. Yang).

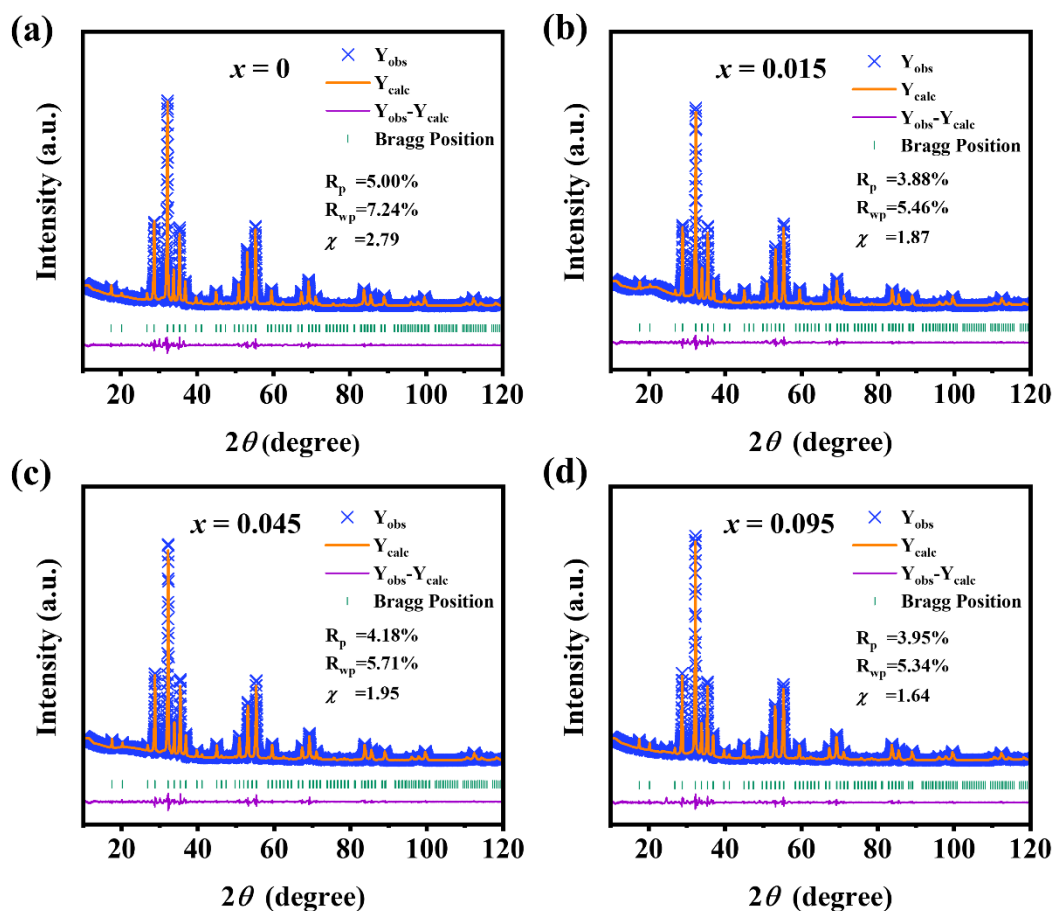


Fig. S1. Rietveld refinement of LCZV: $x\text{Eu}^{3+}$ samples: (a) $x = 0$, (b) $x = 0.015$, (c) $x = 0.045$, and (d) $x = 0.095$.

Table S1. Refined structural data of LCZV: $x\text{Eu}^{3+}$ ($x = 0, 0.015, 0.045, 0.095$) samples.

Sample (x)	a (Å)	V (Å ³)	R_p (%)	R_{wp} (%)	χ^2
0	12.43993(44)	1925.101(117)	5.00	7.24	2.79
0.015	12.43511(37)	1922.866(100)	3.88	5.46	1.87
0.045	12.43721(39)	1923.839(105)	4.18	5.71	1.95
0.095	12.43943(37)	1924.870(99)	3.95	5.34	1.64

Table S2. The atom sites, temperature factors, and atomic occupancy of LCZV: $x\text{Eu}^{3+}$ ($x = 0, 0.015, 0.045, 0.095$) samples.

Atom	Wyck.	x	y	z	Uiso	Occupancy
$x = 0$						
Ca1	24c	0.125	0	0.25	1.895(85)	0.912
Li1	16a	0	0	0	1.265(75)	0.167
Zn1	16a	0	0	0	0.889(75)	0.503
V1	24d	0.375	0	0.25	0.364(62)	0.844
O1	96h	0.03709(19)	0.05314(18)	0.65827(28)	2.309	1
$x = 0.015$						
Ca1	24c	0.125	0	0.25	1.357(77)	0.912
Eu1	24c	0.125	0	0.25	1.357(77)	0.004
Li1	16a	0	0	0	0.794(63)	0.170
Zn1	16a	0	0	0	0.419(63)	0.509
V1	24d	0.375	0	0.25	0.065(56)	0.852
O1	96h	0.03741(17)	0.05534(16)	0.65719(25)	1.615	1
$x = 0.045$						
Ca1	24c	0.125	0	0.25	1.278(84)	0.900
Eu1	24c	0.125	0	0.25	1.278(84)	0.016
Li1	16a	0	0	0	0.906(65)	0.174
Zn1	16a	0	0	0	0.531(65)	0.509
V1	24d	0.375	0	0.25	0.307(82)	0.880
O1	96h	0.03697(18)	0.05444(16)	0.65785(23)	1.554	1
$x = 0.095$						
Ca1	24c	0.125	0	0.25	0.945(86)	0.896
Eu1	24c	0.125	0	0.25	0.945(86)	0.020
Li1	16a	0	0	0	0.927(64)	0.177
Zn1	16a	0	0	0	0.551(64)	0.491
V1	24d	0.375	0	0.25	0.519(88)	0.888
O1	96h	0.03722(17)	0.0545(15)	0.65829(21)	1.644	1

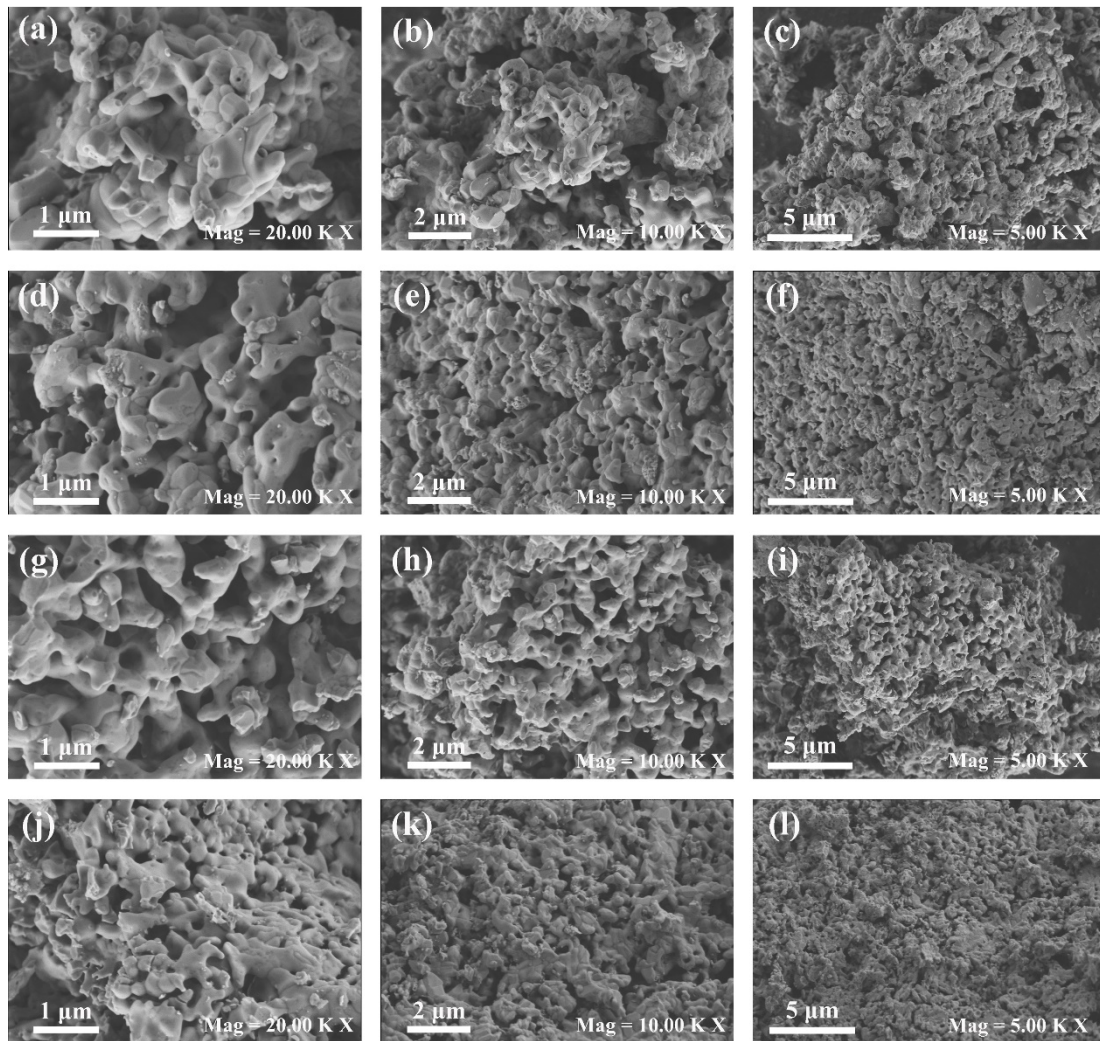


Fig. S2. SEM images of LCZV: $x\text{Eu}^{3+}$ ($x = 0, 0.015, 0.045, 0.095$) collected at different magnifications:

(a-c) LCZV; (d-f) LCZV:0.015Eu³⁺; (g-i) LCZV:0.045Eu³⁺; (j-l) LCZV:0.095Eu³⁺.

Table S3. CIE coordinates of LCZV:xEu³⁺ (x = 0-0.155) samples under 310 nm excitation.

Samples (x)	CIE x	CIE y	Peak	CCT
0.000	0.2039	0.2421	500	64671.4613
0.005	0.2287	0.2648	613	24330.6955
0.010	0.2523	0.2941	613	11340.8941
0.015	0.2739	0.3145	613	7683.2020
0.020	0.2843	0.3243	613	6772.2369
0.030	0.3078	0.3487	613	5748.6597
0.045	0.3282	0.3695	613	5521.4678
0.060	0.3524	0.391	613	5619.6741
0.075	0.3544	0.3922	613	5639.3109
0.095	0.3634	0.4014	613	5736.9235
0.115	0.3438	0.38	613	5555.4173
0.135	0.3444	0.3777	613	5560.4394
0.155	0.3395	0.3711	613	5534.0609

CCT can be calculated by the formula: ¹

$$CCT = 437n^3 + 3601n^2 + 6831n + 5517 \quad (1)$$

where n is the calculation coefficient, x and y are chromaticity coordinates.

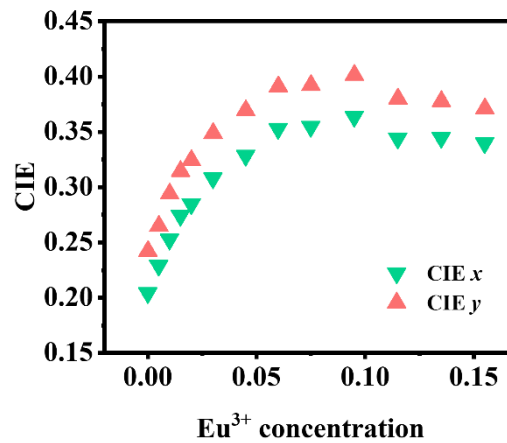


Fig. S3. The relationship between doping concentration and CIE coordinates of LCZV:xEu³⁺ (x = 0-0.155).

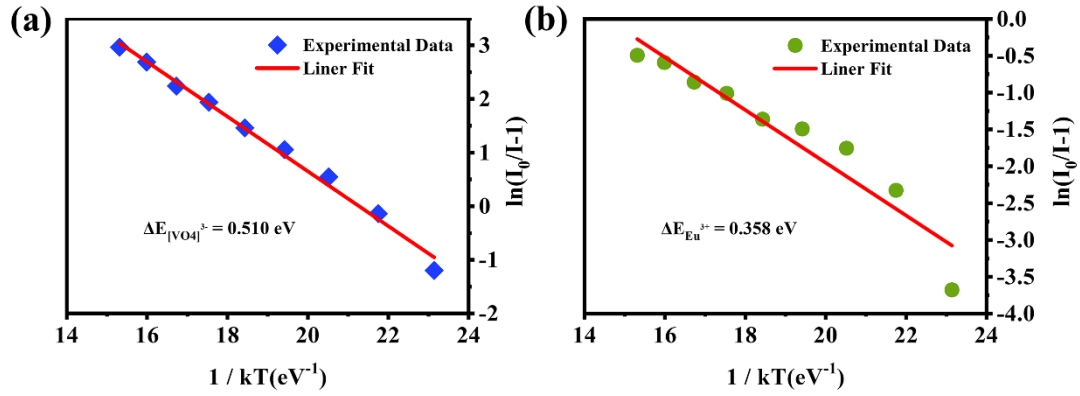


Fig. S4. Arrhenius fitting of temperature-dependent emission intensities of ΔE values for (a) $[VO_4]^{3-}$ and (b) Eu^{3+} in the LCZV:0.015 Eu^{3+} phosphors.

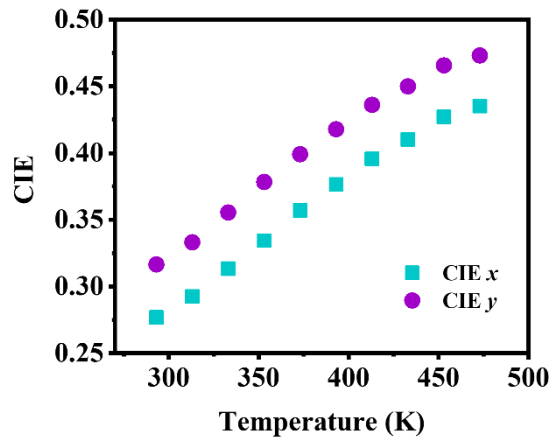


Fig. S5. The relationship between temperature and CIE coordinates of LCZV: xEu^{3+} ($x = 0-0.155$).

References

1. P. Fan, Z. Xu, Q. Luo, Z. He, Y. Chen, Q. Miao, C. Huang, X. Liu and L. Li, *J. Alloys Compd.*, 2021, **885**, 160958.